

# Thermally Induced Structural Changes in $F^-(H_2O)_{11}$ and $Cl^-(H_2O)_{11}$ Clusters: Molecular Dynamics Computer Simulations

Laura S. Sremaniak, Lalith Perera, and Max L. Berkowitz\*

Department of Chemistry, University of North Carolina Chapel Hill, North Carolina 27599

Received: June 9, 1995; In Final Form: July 31, 1995<sup>⊗</sup>

We performed constant energy molecular dynamics computer simulations on  $F^-(H_2O)_{11}$  and  $Cl^-(H_2O)_{11}$  clusters and examined the dependence of ion solvation on temperature. At low temperatures the ion resides on the surface for both  $F^-$  and  $Cl^-$ , but as the clusters are warmed, the  $F^-$  becomes more and more solvated while  $Cl^-$  remains on the surface. Comparing the behavior of  $F^-(H_2O)_{11}$  and  $Cl^-(H_2O)_{11}$  to that of pure  $(H_2O)_{12}$ , we observe that when heating the clusters from their minimum energy configurations, the behavior of the heterogeneous clusters during melting is mostly determined by water–water interactions.

## 1. Introduction

Our understanding of structural and dynamical properties of aqueous solutions is constantly improving due to recent intense work in theory, experiment, and computer simulations.<sup>1</sup> To perform computer simulations on large samples and for long periods of time (of nanosecond order), potential functions are needed to describe the interactions of molecules in the solutions. To test the quality of such functions, we can compare information from experiments on aqueous clusters and simulations performed on the same systems. The advantage of working with clusters in simulations is that artificially imposed periodic boundary conditions and approximate treatment of long-range forces do not exist.

With this in mind we studied the effect of the inclusion of many-body interactions into the description of  $Cl^-(H_2O)_n$  and  $Na^+(H_2O)_n$  clusters.<sup>2</sup> To our surprise we observed that the  $Cl^-$  anion is not solvated in  $Cl^-(H_2O)_n$  even when  $n = 20$ .<sup>3</sup> Later simulations showed that the same behavior is observed in clusters with  $Br^-$  and  $I^-$  ions.<sup>4,5</sup> Calculated photodetachment spectra compared well with the experimental spectra<sup>6</sup> for  $Br^-$  and  $I^-$  ions in water clusters with up to 16 water molecules, thus indicating that indeed these two ions are situated on the surface of water clusters. Photodetachment spectra of  $Cl^-(H_2O)_n$  ( $n = 1–16$ ) were also calculated<sup>7</sup> and showed good agreement with the experimental data which are only available for  $n = 1–7$ .

With respect to structural characteristics of aqueous clusters with an  $F^-$  ion, molecular dynamics simulations of  $F^-(H_2O)_n$  ( $n = 2–15$ ) showed that at temperatures around 200 K the ion was solvated in clusters with more than six water molecules.<sup>8</sup> At 0 K and with  $n = 6–8$ , we observed that the  $F^-$  ion in the lowest energy structures resides on the surface. In the same size clusters with  $Cl^-$ , the ion remained on the surface regardless of temperature. It was therefore proposed that the driving force behind  $F^-$  solvation is entropy.

The purpose of this paper is to further explore the temperature dependence of ion solvation in water clusters. Using molecular dynamics we simulated  $F^-(H_2O)_{11}$  and  $Cl^-(H_2O)_{11}$  clusters to address two specific issues: the first is the difference in the degree of solvation of  $F^-$  versus  $Cl^-$ , and the second is the issue of how they both compare to the reference state of  $(H_2O)_{12}$ .

Larger clusters were chosen for the present study mainly because the degree to which the ion is solvated in them becomes

more pronounced and it is thus easier to detect the structural changes of interest. The decision to simulate a cluster with 11 waters and  $F^-$  or  $Cl^-$  was based in part on the structures that were found in our previous work<sup>8</sup> on  $F^-(H_2O)_7$  and  $Cl^-(H_2O)_7$  and the work in refs 9–11 on clusters of eight waters. In the homogeneous water cluster the lowest energy configuration is cubic with one oxygen atom sitting at each of the eight vertices. For the heterogeneous clusters in their lowest energy minima, the ion replaces one of the waters at one vertex of the cube and there is of course a rearrangement in the hydrogen bonding. A larger size structure containing two cubes could then be realized by adding a tetramer to the cubic octamer. In addition, the choice of simulating a cluster of 11 waters and an ion can further be rationalized when considering that the lowest energy minimum geometry of  $(H_2O)_{12}$  reported in ref 12 is bicubic. In replacing one of the waters by an ion, one might expect that the bicubic geometry remains.

## 2. Methods

Water–water and water–ion interactions are described by the POL1 potential.<sup>13–15</sup> This potential contains a two-body additive part, a polarization term, and a three-body repulsive term. Details about the potential and its ability to give correct structural and dynamical properties when compared with experiments on these systems can be found in ref 8.

To simulate our systems, four sets of equations of motion were solved for each water molecule and two sets for the ion. Center of mass positions and center of mass velocities were propagated using Newton's equation of motion, and angular velocities were propagated with Euler equations of motion. The final set of four equations describe the propagation of the molecular orientations themselves. Each rigid water was assigned a set of four quaternion parameters, which became the generalized coordinates for orientation.<sup>16</sup> These four parameters are not mutually independent and must be normalized at each step of the trajectory. The equations of motion were integrated using a sixth-order Gear predictor–corrector algorithm<sup>17,18</sup> in order to achieve good energy conservation (the drift in energy was less than 0.04% over 500 ps). In all cases a 0.5 fs time step was used. The induced dipoles were calculated iteratively with a tolerance of  $1.0 \times 10^{-8}$ , which is stricter than in previous simulations.<sup>8</sup>

Both  $F^-(H_2O)_{11}$  and  $Cl^-(H_2O)_{11}$  were run at high temperatures (greater than 200 K) for 1 ns and at intervals of 5 ps configurations were saved and quenched by periodically remov-

<sup>⊗</sup> Abstract published in *Advance ACS Abstracts*, December 15, 1995.

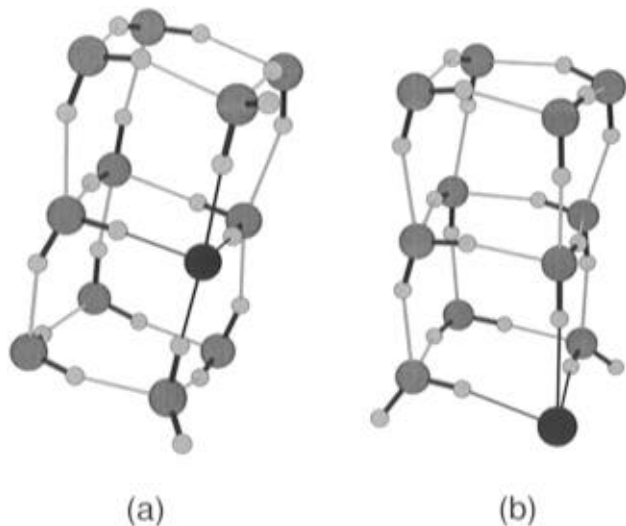


**Figure 1.** Geometries of the lowest energy minimum of (a)  $F^-(H_2O)_{11}$  and (b)  $Cl^-(H_2O)_{11}$ . The ion is black, and thin dark lines from ion to hydrogens are only a viewing aid. Hydrogen bonds are shown as lighter thin lines. Hydrogen bonds are drawn if the distance between the hydrogen and neighboring oxygen is less than or equal to 2.4 Å.

ing the kinetic energy. This procedure produced many clusters in their local minimum energy configurations. To investigate what effect temperature has on the structure, we performed the heating procedure on both  $F^-(H_2O)_{11}$  and  $Cl^-(H_2O)_{11}$  clusters, which had the lowest energies among the quenched configurations. The increase in total energy was achieved by adding kinetic energy through the assignment of initial velocities to the particles of the clusters. At each successively higher total energy, however, we kept the initial positions to be the same as those of the energy minima. The increment in kinetic energies was asystematic but chosen to produce a set of clusters with a variety of energies. More clusters of intermediate energies were needed to characterize to onset of melting. The total linear and angular momenta were removed at the beginning of each run, and the cluster was equilibrated for 30 ps. All production runs were 500 ps in length.

It should be noted that heating runs were chosen instead of cooling since it is easier to establish transition temperatures with melting rather than freezing due to the stochastic nature of nucleation in freezing making the transition temperature irreproducible.<sup>19</sup>

### 3. Results

**3.1. Minimum Energy Structures.** Compared to earlier simulations with  $F^-(H_2O)_7$  and  $Cl^-(H_2O)_7$ , where we observed that the minimum energy structures are cubic,<sup>8</sup> the minimum energy structures for both  $F^-(H_2O)_{11}$  and  $Cl^-(H_2O)_{11}$  (Figure 1) show a similar geometry in that the ion is sitting on the edge of a dodecamer which is a double cube. The  $F^-$  ion occupies a middle position, where it has four water neighbors, whereas the  $Cl^-$  ion sits in the corner with only three neighboring waters. The  $F^-(H_2O)_{11}$  double cube is slightly more distorted due to the larger ion–water interaction as compared to the cube with the chloride anion.

The geometry of the observed dodecamer can be rationalized in terms of a fusion of an octamer containing seven waters and an ion (which has a cubic minimum energy geometry) with a water tetramer (of a cyclic square shape). The water tetramer can merge on the side of the octamer where the ion resides, as happens in the case of fluoride, or it can merge on the opposite side of the octamer, as happens in the case of chloride. A similar kind of behavior was observed in previous simulations where

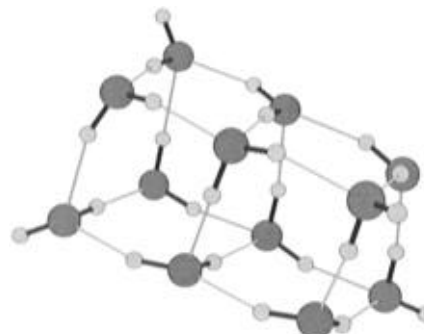


**Figure 2.** Minimum energy geometry of  $(H_2O)_{12}$ .

one water was added to the octamer containing either the  $F^-$  ion or the  $Cl^-$  ion.<sup>8</sup> Despite this comparison, we cannot with absolute certainty say these bicubic structures are the global minima.

As noted above, a cluster of 12 waters also is predicted to have a double-cube structure at its lowest energy minimum<sup>11b,12</sup> (Figure 2), and it is to this structure that comparisons are made. This structure has 20 hydrogen bonds and  $-463.5$  kJ/mol of total energy, whereas the  $F^-$  double cube has 16 hydrogen bonds and a total energy of  $-727.4$  kJ/mol; the  $Cl^-$  double cube, 17 hydrogen bonds and  $-612.4$  kJ/mol of total energy. The large difference in energy in the pure water double cube and the double cube with an ion can be understood in terms of the large ion–water interactions: they are approximately  $-100$  kJ/mol for  $F^-$ –water and  $-60$  kJ/mol for  $Cl^-$ –water, whereas the water–water interaction for this model is only  $-23$  kJ/mol on the average.

**3.2. Melting.** Questions related to phase behavior, melting, and freezing of small homogeneous clusters were addressed recently in detail.<sup>11,20–27</sup> Since our goal here is to study the change in the structure of the clusters  $F^-(H_2O)_{11}$  and  $Cl^-(H_2O)_{11}$  with the change in temperature, we address the issue of the melting of these clusters only in the aspect related to structural change.

What happens to these ion–water clusters as they are heated? Using the Moviemol program<sup>28</sup> to view the dynamics of the clusters, we observe that in the low-energy regime the ion and water molecules vibrate around the same positions as in their minimum energy configurations. As the energy is raised, more and more hydrogen bonds are broken. In the intermediate energy regime half of the double cube breaks apart, while the other half retains its hydrogen-bonded cubic structure. At even higher energies all waters and the ion are free to move. But the way in which the ion changes its position with the cluster upon heating is strikingly different. When the cluster with  $F^-$  acquires enough energy to start breaking hydrogen bonds, the waters begin to surround the ion on all sides. In the intermediate region of energy, the ion can fluctuate between surface and interior positions. At even higher energies the ion becomes more solvated than nonsolvated. The cluster with  $Cl^-$  behaves differently upon heating. More waters surround the ion, but the solvation remains one-sided even at high energies. Snapshots of high-energy configurations of both  $F^-$  and  $Cl^-$  systems taken from these movies are shown in Figure 3.

Determining the onset of melting was accomplished in several ways. First, according to the Lindemann criterion,<sup>29</sup> the onset of melting occurs when there is a large change in the value of the root mean square bond length fluctuation defined as

$$\delta = \frac{1}{M} \sum_{i < j}^n \frac{(\langle r_{ij}^2 \rangle - \langle r_{ij} \rangle^2)^{1/2}}{\langle r_{ij} \rangle} \quad (1)$$

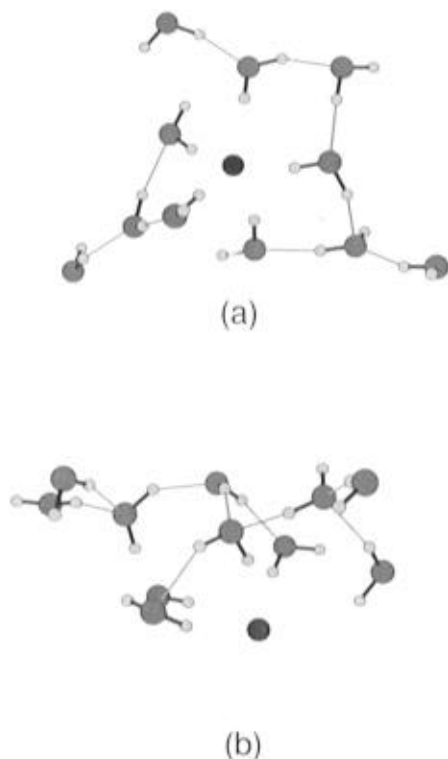


**Figure 3.** Snapshots of (a)  $F^-(H_2O)_{11}$  at  $T = 239$  K and (b)  $Cl^-(H_2O)_{11}$  at  $T = 230$  K. The same convention as in Figure 1 is used for hydrogen bonds, but no connecting lines to the ion are shown.

In this equation,  $r_{ij}$  is the distance between oxygen atoms  $i$  and  $j$  in the case of  $\delta_{OO}$  and the distance between the oxygen and the ion in the case of  $\delta_{O-ion}$ , and  $M$  is the number of  $ij$  pairs. Both  $\delta_{OO}$  and  $\delta_{O-ion}$  are plotted in Figures 4a and 5a. For clusters with  $F^-$  this large change happens at an energy of  $-632.6$  kJ/mol, which is 94.8 kJ/mol above the minimum energy, and for clusters with  $Cl^-$  at  $-510.5$  kJ/mol, or 101.9 kJ/mol above its energy minimum. The curves of the root mean square bond length fluctuations for oxygen–oxygen and oxygen–ion parallel each other for both  $F^-$  and  $Cl^-$ , and in both cases  $\delta_{OO}$  is greater than  $\delta_{O-ion}$ , indicating that more of the motion is coming from the waters.

Caloric curves were drawn for both water–ion clusters (Figures 4b and 5b). They show the change in temperature with total energy. For the cluster with  $F^-$ , a break in the caloric curve occurs at  $-632.6$  kJ/mol and for the cluster with  $Cl^-$  at  $-510.5$  kJ/mol, which indicates the beginning of the solid–liquid coexistence region. Note that these are exactly the same energies where  $\delta_{OO}$  experiences a large change. The curves then level out again once they reach the liquid-like region. Taking the energies where the coexistence region begins and ends from the root mean square bond length fluctuation curve and finding the corresponding temperatures from the caloric curve give the temperature range over which melting occurs. The range of melting in  $F^-$  was 150–180 K, while for  $Cl^-$  it is 157–187 K. Such a similar range of melting suggests that the ion's role is small and that the water–water interactions are determining when and how the cluster melts.

The third panel in these figures shows the change in coordination number with change in energy for each cluster. In Figures 4c and 5c the curves display a break in the transition region, and this break occurs at energies similar to those in Figures 4a,b and 5a,b. Coordination numbers will be further discussed below.

Another criterion which characterizes melting is the change in the behavior of the mean square displacement curves. Figure

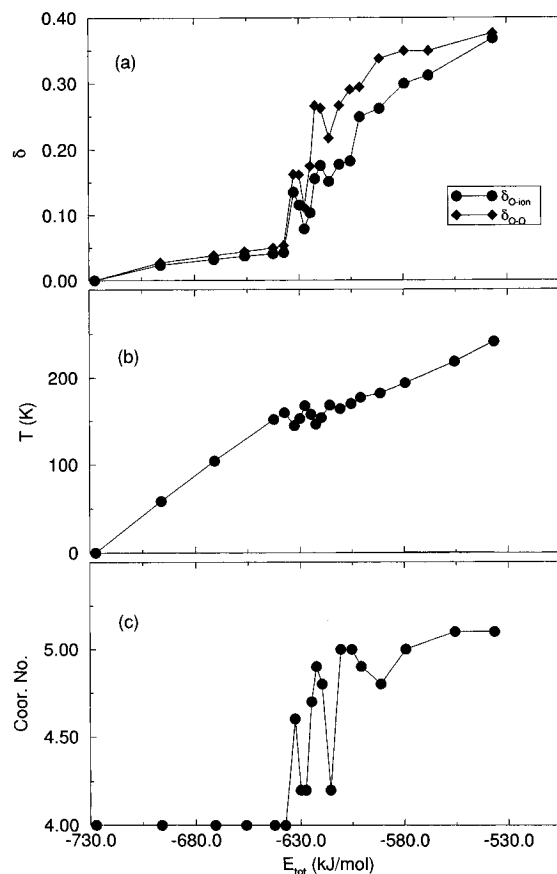


**Figure 4.** (a) Root mean square bond length fluctuations, (b) caloric curve, and (c) coordination numbers for  $F^-(H_2O)_{11}$ .

6 shows how the mean square displacement changes in going from the solid-like to liquid-like regions. From this figure we observe that the mean square displacement of water in solid-like  $F^-(H_2O)_{11}$  and  $Cl^-(H_2O)_{11}$  clusters is not changing with time, indicating little diffusion. The diffusion gets increasingly larger at higher energies. For the highest energy simulated, the diffusion coefficient of water was  $2.02 \times 10^{-5}$  cm<sup>2</sup>/s in both  $Cl^-(H_2O)_{11}$  (at 230 K) and  $F^-(H_2O)_{11}$  (at 239 K). (Compare this with the diffusion coefficient of liquid water under the same model at 300 K, which is  $3.1 \times 10^{-5}$  cm<sup>2</sup>/s.<sup>14</sup>) The same diffusion coefficient for both ion–water clusters supports the idea that their behavior in the liquid-like region is similar and ion-independent.

To test the dependence of melting on the starting configuration for the heating procedure, we selected another  $F^-(H_2O)_{11}$  cluster with a local minimum ( $-686.4$  kJ/mol, see Figure 7 for this cluster's structure) occurring often among the quenched structures and heated it. (Hereafter this cluster is referred to as F2; the one heated from the lowest minimum energy, as F1.) The root mean square bond length fluctuations (Figure 8) show an immediate increase after  $-666.1$  kJ/mol or 57 K, which is at a much lower temperature than in the F1 case. At 100 K, F2 would be in the coexistence region, while the F1 cluster would still be solid-like. The caloric curve for F2 is shown in Figure 9 with squares along with the caloric curves for the other two systems which were previously discussed and the caloric curve for the pure water cluster discussed below. This curve shows that the temperature range (which is 57–167 K) as well as the energy range of coexistence for F2 is greater in magnitude than in the F1 cluster. In the liquid-like region the F1 and F2 curves merge into one.

To compare the melting behavior of the clusters with an ion present to a cluster with no ion present, a simulation was done

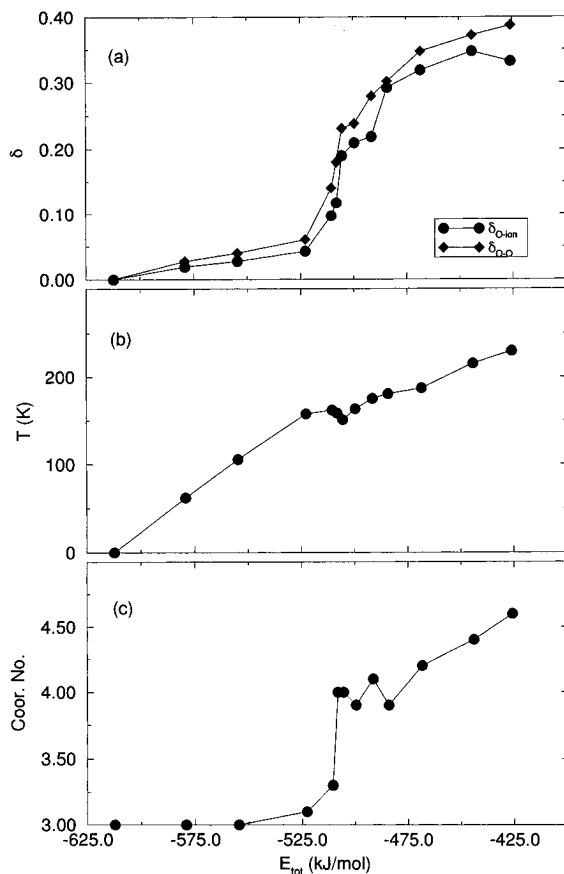


**Figure 5.** (a) Root mean square bond length fluctuations, (b) caloric curve, and (c) coordination numbers for  $Cl^-(H_2O)_{11}$ .

on an  $(H_2O)_{12}$  cluster. The starting configuration was the one given in ref 12 as the lowest minimum energy dodecamer, which is a double cube. This configuration was artificially made. Farantos et al.<sup>12</sup> also prepared this minimum energy structure and never found it through quenching from a hot water cluster, although other cubic forms of the dodecamer were found to be minima. Starting from the minimum energy configuration, a heating run was performed using the same protocol as for the ion-water clusters. The root mean square bond length fluctuations are plotted in Figure 10. A large increase in  $\delta_{OO}$  after  $-381.9$  kJ/mol clearly indicates the beginning of the coexistence region, which ends at  $-335.6$  kJ/mol. The caloric curve corresponding to this dodecamer shown in Figure 9 as diamonds also indicates that melting occurs in this region, but the break in the curve is not nearly as distinct as it is in Figure 10. In Figure 9, the data points of total energy which bracket the coexistence region correspond to a temperature range 121–181 K. This range includes the transition temperature reported earlier in ref 12 of 170 K.

The slopes of the first portion of the caloric curves for  $F1$ ,  $Cl^-(H_2O)_{11}$ , and  $(H_2O)_{12}$  all have a similar value (approximately 1.8 K/(kJ/mol)). This indicates that the behavior of these clusters in the solid phase is very similar, which is expected considering their similar geometry. In the liquid-like region the caloric curves of the three clusters have slopes of 1.03, 0.84, and 1.14 K/(kJ/mol), which correspond to heat capacities of 81, 99, and 73 J/(mol K), respectively. (Note that liquid water's experimental heat capacity at 298 K is 75.3 J/(mol K).) The similarity in the heat capacities of the three clusters is another indication that the behavior of the clusters is mostly determined by water.

**3.3. Solvation and Hydrogen-Bonding Network.** The difference in the degree of solvation at different energies can

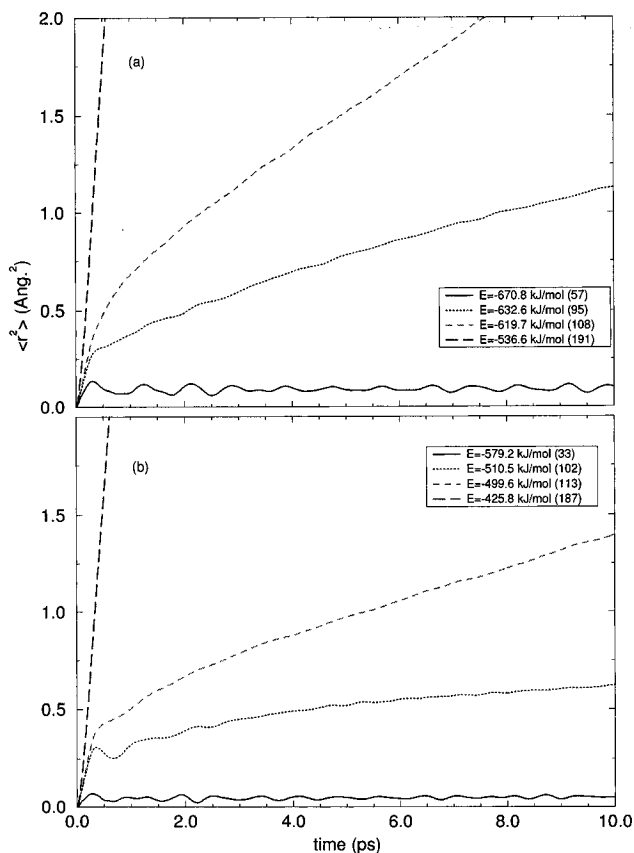


**Figure 6.** Mean square displacement curves at four energies, where energy is reported as total energy and in parentheses as units above the minimum energy. The curve represented by the solid line is in the solid-like region, the middle two are in the coexistence region, and the long dashed line is in the liquid-like region: (a)  $F^-(H_2O)_{11}$ ; (b)  $Cl^-(H_2O)_{11}$ .

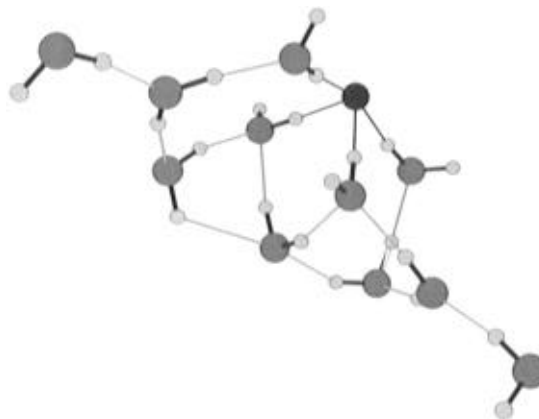


**Figure 7.** Geometry of a selected higher energy minimum of  $F^-(H_2O)_{11}$  (F2).

be evaluated quantitatively in several ways. One way is to calculate the angular distribution function, the plot of which is presented in Figure 11 for  $F1$  and  $Cl^-(H_2O)_{11}$ . The angular distribution function represents a distribution of the cosine of the angle between the vector connecting the oxygen atoms of the neighboring water molecules to the ion and the vector from the ion to the center of mass of the whole cluster. Therefore, the flatness of the curve indicates the degree to which the ion is surrounded by waters; a curve with zero slope would thus be evidence of full ion solvation. At low energies for  $F1$  and  $Cl^-(H_2O)_{11}$  clusters the graph shows two distinct peaks which merge into one continuous distribution at higher energies. In

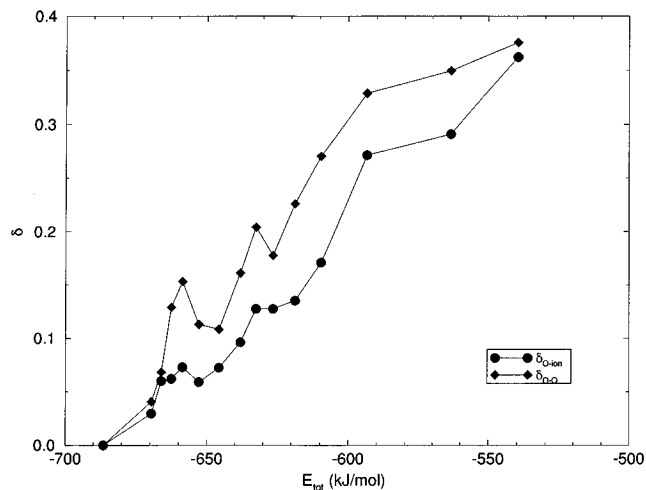


**Figure 8.** Root mean square bond length fluctuations for F2.

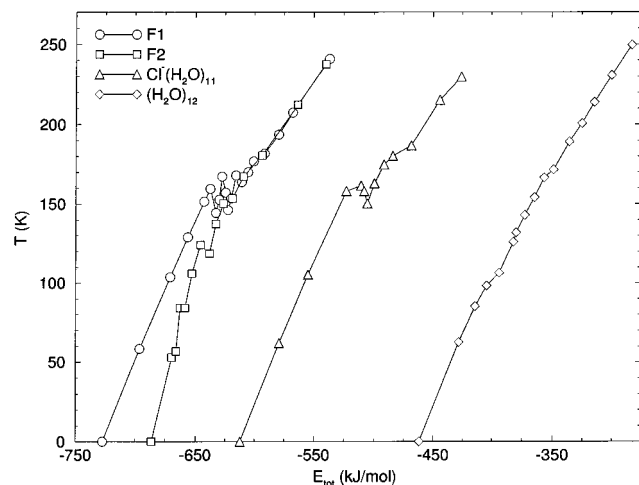


**Figure 9.** Caloric curves for  $\text{Cl}^-(\text{H}_2\text{O})_{11}$ ,  $(\text{H}_2\text{O})_{12}$ , and both  $\text{F}^-(\text{H}_2\text{O})_{11}$  clusters.

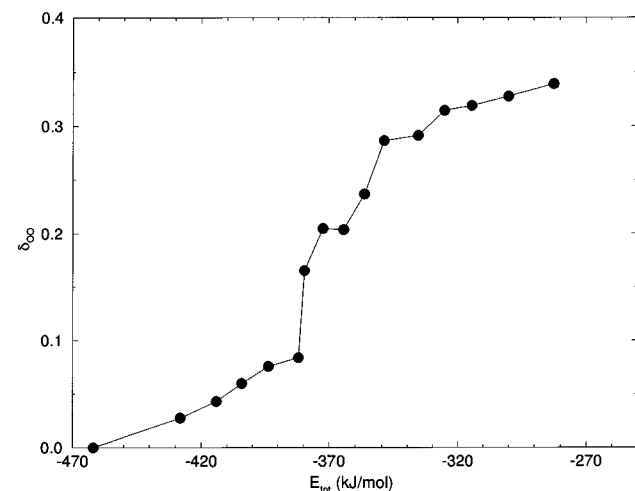


**Figure 10.** Root mean square bond length fluctuations for  $(\text{H}_2\text{O})_{12}$ .

the liquid-like regime the curve of F1 is flatter than that of  $\text{Cl}^-(\text{H}_2\text{O})_{11}$ , indicating a higher degree of ion solvation.

That the  $\text{F}^-$  ion in the F1 cluster becomes more solvated than  $\text{Cl}^-$  upon heating can also be seen in the plots of the distributions of the distances from the ion to the center of mass of the cluster (Figure 12). In the minimum energy structure the  $\text{F}^-$  ion is about 2.1 Å from the center of mass and gradually moves closer to the center of mass upon heating.  $\text{Cl}^-$  starts off further away (3.6 Å) from the center of mass, as it is in the corner of the

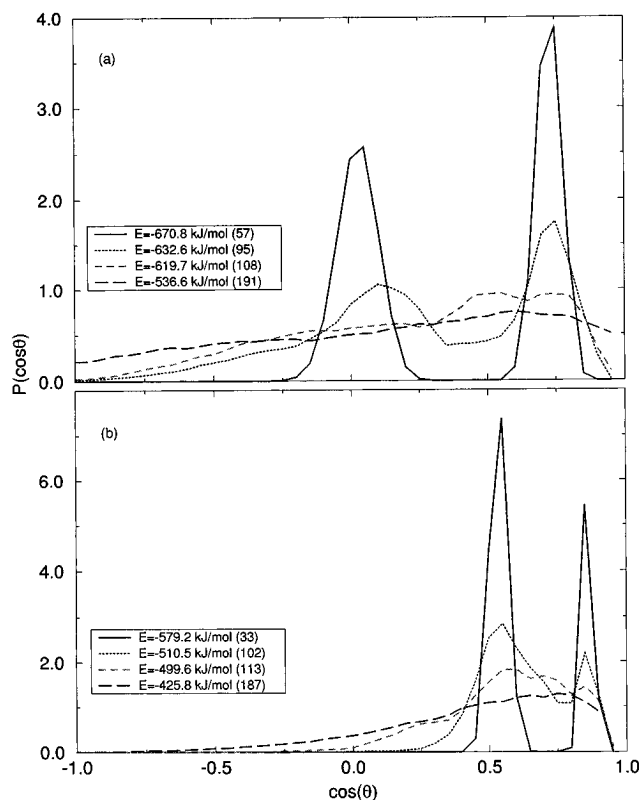


**Figure 11.** (a) Angular distribution functions for F1 at the same four energies as in Figure 6. (b) Same as (a) but for  $\text{Cl}^-(\text{H}_2\text{O})_{11}$ .

cube and moves in as the waters surround it on one side, but on the average it remains 1 Å further from the center of mass than  $\text{F}^-$  does.

Coordination numbers provide another way of characterizing solvation before and after melting. They were calculated by counting the average number of waters around the ion up to the first minimum of the radial distribution function at each energy. The coordination number of  $\text{F}^-$  (in F1, see Figure 4c), initially at 4, fluctuates in the transition region and then reaches a value greater than 5 after melting. Low coordination numbers in the coexistence region indicate that the cluster is trapped in a solid-like configuration. The coordination number for  $\text{Cl}^-$  (Figure 5c) starts at 3 and ends up at 4.5, with little fluctuation as it is heated. It is hard to discriminate structural properties by looking at coordination numbers alone, especially in the transition region, where the clusters can reside in a solid-like or a liquid-like region of phase space for a while and, in addition, the sheer number cannot describe the placement of the waters around the ion.

To connect melting to structural changes, it is instructive to analyze the hydrogen-bonding patterns shown in Figures 13, 14, and 15. Hydrogen bonds were counted if they met two criteria: first, that the distance between the hydrogen and the neighboring water oxygen is less than 2.5 Å and, second, that the  $\text{OH}\cdots\text{O}$  angle is greater than  $120^\circ$ , where the first O is the covalently bonded oxygen and the second is a neighboring oxygen. From these figures we observe that up to and after the transition region the hydrogen-bonding pattern is monotonic, while in the transition region, the pattern is random. In the liquid-like region, compare the hydrogen bonds of the first shell of waters around the fluoride ion (in the F1 cluster shown in Figure 13a) to those in the same shell in the chloride-water cluster (Figure 14a). For both clusters, most of the hydrogen bonding can be accounted for by the number of one and two hydrogen bonds per water molecule, but in the case of the cluster

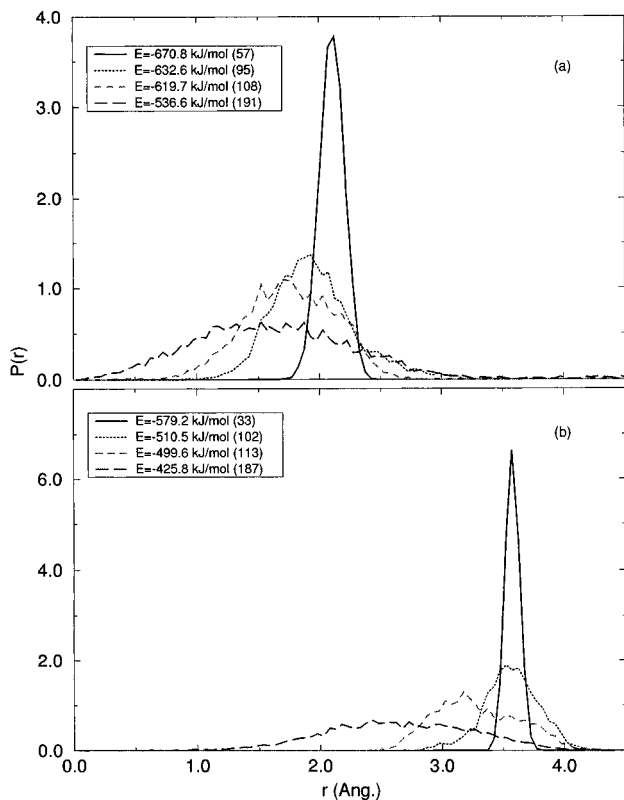


**Figure 12.** (a) Ion to center of mass distance distributions for F1 at the same four energies as in Figure 6. (b) Same as (a) but for  $Cl^-(H_2O)_{11}$ .

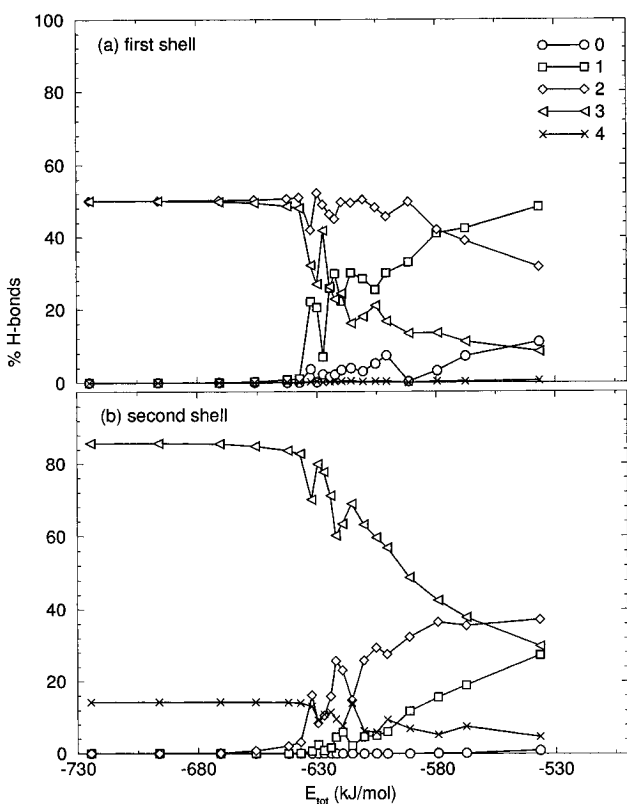


**Figure 13.** Hydrogen-bonding patterns for the F1 cluster reported as percentage of zero, one, two, three, and four hydrogen bonds per water molecule: (a) first shell; (b) second shell.

with  $F^-$ , the percentage of one hydrogen bond is greater than that of two; however, in the cluster with  $Cl^-$ , it is just the opposite. This indicates that waters in the F1 case have a slightly more disrupted hydrogen-bonded network next to the

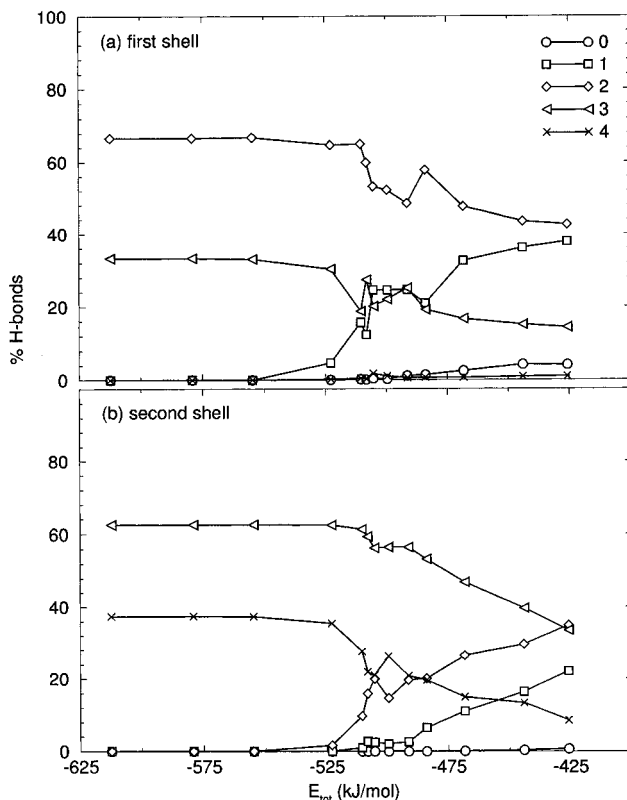


**Figure 14.** Hydrogen-bonding patterns for  $Cl^-(H_2O)_{11}$ : (a) first shell; (b) second shell.

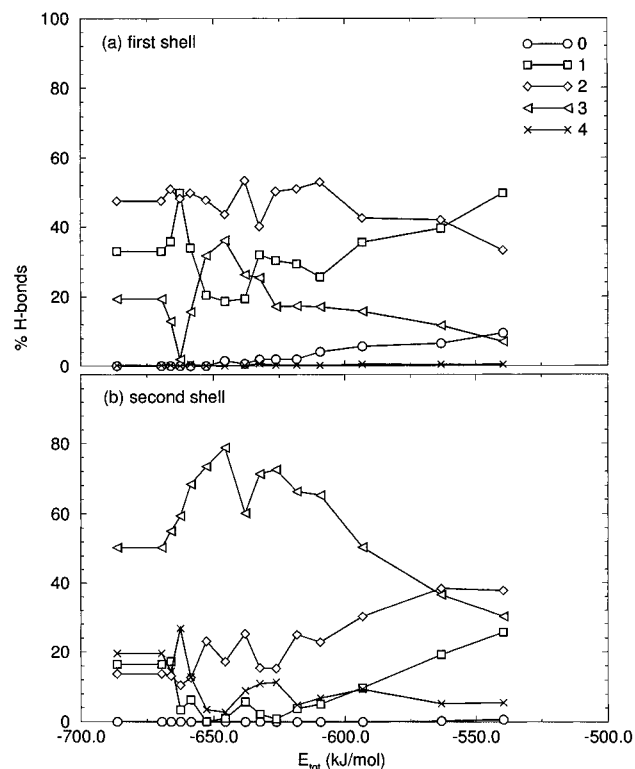


**Figure 15.** Hydrogen-bonding patterns for the F2 cluster: (a) first shell; (b) second shell.

ion, whereas in the  $Cl^-(H_2O)_{11}$  case, they are more hydrogen bonded to each other. In the second shell (Figures 13b and 14b) there is not much difference in these two clusters: the percentage of one or two hydrogen bonds increases and that of three and four decreases in much the same way for both clusters as the energy increases. The similar hydrogen-bonding pattern

for the second shell supports the above suggestion that the water network is more responsible for melting.

In comparing the first shells of water in two different  $F^-(H_2O)_{11}$  clusters (Figures 13a and 15a), the major differences are seen in the solid-like region, where the F2 cluster has more of a balance between one, two, and three hydrogen-bonded waters, whereas two and three hydrogen-bonded waters are the only ones present in the double-cube structure. The F2 cluster does not have a structured hydrogen bond network to break before it can melt, as the F1 cluster must do. At high energies, the hydrogen-bonding pattern for the first shells of F1 and F2 are similar, as are the patterns for their second shells. The similarity at high energies was also seen in the caloric curves for these two clusters.

#### 4. Conclusion

Using molecular dynamics simulations we studied the structural and dynamical properties of  $F^-(H_2O)_{11}$  and  $Cl^-(H_2O)_{11}$  clusters as a function of temperature. From the simulations we concluded that at 0 K the lowest minimum energy structure of each cluster is a double cube and the ion is sitting on the edge of the cube. The  $F^-$  ion occupies a middle position, where it has four water neighbors, whereas the  $Cl^-$  ion sits in the corner, with only three water neighbors.

As the clusters are heated, they begin to melt. When starting from the lowest minimum energy configuration, the melting of the double cube is similar no matter which ion is involved. This implies that the behavior of the cluster during melting is mostly determined by water–water rather than by water–ion interactions. Evidence of this can be seen from the comparison of the caloric curves of the ion–water clusters to that of the pure water cluster and from the change in the hydrogen-bonding pattern with energy.

In terms of structural differences the  $F^-$  ion becomes more solvated upon melting, while the  $Cl^-$  ion remains on the surface of the cluster. Finally, the onset of melting occurs at different temperatures depending on the starting configuration of the cluster. That may explain why, despite low temperatures achieved in supersonic beams, molecular clusters are not always generated in solid-like states.

**Acknowledgment.** This work was supported by a grant from the Office of Naval Research. Thanks to Dr. U. Essmann for help with the manuscript.

#### References and Notes

- (1) See for example: Friedman, H. L.; Raineri, F. O.; Hirata, F.; Perng, B. C. *J. Stat. Phys.* **1995**, *78*, 1, and references therein.
- (2) Perera, L.; Berkowitz, M. L. *J. Chem. Phys.* **1991**, *95*, 1954; *Ibid.* **1993**, *99*, 4236.
- (3) Perera, L.; Berkowitz, M. L. *J. Chem. Phys.* **1992**, *96*, 8288.
- (4) Sremaniak, L. S.; Perera, L.; Berkowitz, M. L. *Chem. Phys. Lett.* **1994**, *218*, 377.
- (5) Dang, L. X.; Garrett, B. C. *J. Chem. Phys.* **1993**, *99*, 2972.
- (6) Markovich, G.; Pollack, S.; Gingier, R.; Cheshnovsky, O. *J. Chem. Phys.* **1994**, *101*, 9344.
- (7) Perera, L.; Berkowitz, M. L. *J. Chem. Phys.* **1993**, *99*, 4223.
- (8) Perera, L.; Berkowitz, M. L. *J. Chem. Phys.* **1994**, *100*, 3085.
- (9) Bink, G.; Glasser, L. *J. Phys. Chem.* **1984**, *88*, 3412.
- (10) Kim, K. S.; Dupuis, M.; Lie, G. C.; Clementi, E. *Chem. Phys. Lett.* **1986**, *131*, 7766.
- (11) (a) Tsai, C. J.; Jordan, K. D. *J. Chem. Phys.* **1991**, *95*, 3850. (b) Tsai, C. J.; Jordan, K. D. *J. Phys. Chem.* **1993**, *97*, 5208.
- (12) Farantos, S. C.; Kapetanakis, S.; Vegiri, A. *J. Phys. Chem.* **1993**, *97*, 12159.
- (13) Dang, L. X.; Rice, J. E.; Caldwell, J. W.; Kollman, P. A. *J. Am. Chem. Soc.* **1991**, *113*, 2481.
- (14) Caldwell, J. W.; Dang, L. X.; Kollman, P. A. *J. Am. Chem. Soc.* **1990**, *112*, 9144.
- (15) Dang, L. X. *J. Chem. Phys.* **1992**, *96*, 6970.
- (16) Evans, D. J.; Murad, S. *Mol. Phys.* **1977**, *34*, 327.
- (17) Gear, C. W. *Report ANL 7126*; Argonne National Laboratory, 1966.
- (18) Gear, C. W. *Numerical Initial Value Problems in Ordinary Differential Equations*; Prentice Hall: Englewood Cliffs, NJ, 1971.
- (19) Xu, S.; Bartell, L. S. *J. Phys. Chem.* **1993**, *97*, 13550.
- (20) Berry, R. S.; Beck, T. L.; Davis, H. C.; Jellinek, J. *Adv. Chem. Phys.* **1988**, *70b*, 75.
- (21) Berry, R. S. *Chem. Soc. Faraday Trans.* **1990**, *86*, 2343.
- (22) Wales, D. J.; Ohmine, I. *J. Chem. Phys.* **1993**, *98*, 7245.
- (23) Wales, D. J.; Ohmine, I. *J. Chem. Phys.* **1993**, *98*, 7257.
- (24) Del Mistro, G.; Stace, A. J. *J. Chem. Phys.* **1993**, *99*, 4656.
- (25) Wright, D.; El-Shall, M. S. *J. Chem. Phys.* **1994**, *100*, 3791.
- (26) Vegiri, A.; Farantos, S. C. *J. Chem. Phys.* **1993**, *98*, 4059.
- (27) Lynden-Bell, R. M.; Wales, D. J. *J. Chem. Phys.* **1994**, *101*, 1460.
- (28) Hermansson, K.; Ojamae, L. *Report UUIC-B19-500*; University of Uppsala, Institute of Chemistry: Uppsala, 1994.
- (29) Lindemann, F. A. *Z. Phys.* **1910**, *11*, 609.

JP951593G